Check for
updates

Morphology of the Bony Labyrinth Supports the Affinities of *Paradolichopithecus* with the Papionina

Anne Le Maître[1,2] · Franck Guy[2] · Gildas Merceron[2] ·
Dimitris S. Kostopoulos[3]

Abstract

Discoveries in recent decades indicate that the large papionin monkeys *Paradolipo-pithecus* and *Procynocephalus* are key members of the Late Pliocene – Early Pleisto-cene mammalian faunas of Eurasia. However, their taxonomical status, phylogenetic relationships, and ecological profile remain unclear. Here we investigate the two latter aspects through the study of the inner ear anatomy, as revealed by applying micro-CT scan imaging techniques on the cranium LGPUT DFN3-150 of *Paradolichopithecus* from the lower Pleistocene (2.3 Ma) fossil site Dafnero-3 in Northwestern Greece. Using geometric morphometric methods, we quantified shape variation and the allo-metric and phylogenetic signals in extant cercopithecines ($n = 80$), and explored the morphological affinities of the fossil specimen with extant taxa. LGPUT DFN3-150 has a large centroid size similar to that of baboons and their relatives. It shares sev-eral shape features with Macacina and Cercopithecini, which we interpret as prob-able retention of a primitive morphology. Overall, its inner ear morphology is more consistent with a stem Papionini more closely related to Papionina than Macacina, or to a basal crown Papionina. Our results, along with morphometrical and ecological features from previous studies, call into question the traditional hypothesis of a *Para-dolichopithecus*-Macacina clade, and provide alternative perspectives in the study of Eurasian primate evolution during the late Neogene-Quaternary.

Handling Editor: Joanna M. Setchell

✉ Anne Le Maître
  anne.le.maitre@univie.ac.at

1   Department of Evolutionary Biology, University of Vienna, Djerassiplatz 1, 1030 Vienna, Austria

2   PALEVOPRIM – UMR 7262 CNRS INEE, Université de Poitiers, Poitiers, France

3   Laboratory of Geology and Palaeontology, Aristotle University of Thessaloniki, Thessaloniki, Greece

Introduction

At the dawn of the Quaternary and as the Pliocene forests shrank in favor of Pleistocene grasslands under successively cooler climatic conditions (e.g., Popescu *et al.*, 2010), a remarkably homogeneous mammal fauna appears across Eurasia. Stenonoid horses, leptobovines, gazelles, and a variety of cervids are associated with machairodontines, running hyaenas, and raccoon-dogs, the latter species soon replaced by dog-like carnivores (e.g., Aguirre *et al.*, 1994; Agusti & Antón, 2002; Hermier *et al.*, 2020; Koufos, 2001; Koufos *et al.*, 2020; Qiu *et al.*, 2004; Sotnikova & Rook, 2010). Within this transitional context, primates are represented by the supposedly forest-dependent macaques (genus *Macaca* Lacépède, 1799) and the presumed open-dweller large monkeys referred to the genera *Procynocephalus* Schlosser, 1924 and *Paradolichopithecus* Necrasov, Samson, & Radulesco, 1961.

The Late Pliocene to Early Pleistocene taxon *Procynocephalus* was the first fossil primate described; but it is still poorly known, mainly from China and India (Baker & Durand, 1836; Szalay & Delson, 1979; Takai *et al.*, 2014). *Paradolichopithecus*, in contrast, is recorded in France, Spain, Romania, Serbia, Greece, Tajikistan, and China (Eronen & Rook, 2004; Kostopoulos *et al.*, 2018; Radović *et al.*, 2019; Szalay & Delson, 1979 and ref. therein) and its emergence appears to predate that of *Procynocephalus*, with the earliest occurrences being dated around 3.2 Ma. Both genera experienced the maximum of their geographic distribution during the same time interval (ca. 3.0–2.0 Ma), and across the same Eurasian latitudinal belt (roughly within 35°–45°; Takai *et al.*, 2008: Fig. 7). Some authors hypothesize they are synonymous (e.g., Kostopoulos *et al.*, 2018; Nishimura *et al.*, 2010 and ref. therein); others stress, however, the paucity of the available material for formal decisions (e.g., Jablonski, 2002; Szalay & Delson, 1979). Both genera are traditionally considered as representing large macacinans (Delson & Frost, 2004; Strasser & Delson, 1987), although other authors propose closer phylogenetic affinities with the African baboons (Jolly, 1967; Kostopoulos *et al.*, 2018; Maschenko, 1994; Takai *et al.*, 2008).

The estimated body mass of *Paradolichopithecus* (ca. 17 kg for females and 40 kg for males; Kostopoulos *et al.*, 2018: Fig. 10) significantly exceeds known ranges of fossil and extant *Macaca*, indicating this taxon entered into novel size classes, comparable to those of extant baboons and relatives. An evolutionary increase in body size is reported to be the main force toward new cranial shape patterns gained allometrically in Papionina (Frost *et al.*, 2003; Gilbert & Rossie, 2007; Gilbert *et al.*, 2009; Joganic & Heuzé, 2019; Joganic *et al.*, 2018; Leigh, 2006; Leigh *et al.*, 2003; Monson *et al.*, 2017; Nishimura *et al.*, 2019; Profico *et al.*, 2017; Singleton, 2002). Large size in *Paradolichopithecus* is associated with specific postcranial adaptations (e.g., Sondaar *et al.*, 2006; Szalay & Delson, 1979; Ting *et al.*, 2004; van der Geer & Sondaar, 2002) highlighting a terrestrial way of life comparable to that of baboons, and in accordance with available information from dental tissue (Plastiras, 2021; Williams & Holmes, 2012). Whether, however, this common path to increased size and terrestrial behaviors reflects

close phylogenetic relationships between *Paradolichopithecus* and baboons or it simply represents an example of parallelism still has to be tested.

Given the persistent controversy about the phylogenetic position of *Paradolichopithecus*, the importance of the evidence coming from phylogenetically informative anatomical areas is paramount. In vertebrates, the inner ear is involved in many functions: hearing, balance, posture control, and gaze stabilization (e.g., Graf & Klam, 2006). The cochlear system enables sound perception, while the vestibular system detects head movements and accelerations (Fig. 1). The vestibular system corresponds to the semicircular canal system and the vestibule. The semicircular canal system in composed of the lateral, anterior, and posterior semicircular canals (respectively LSC, ASC and PSC), the two latter being connected at the common crus. The circular movements of the head are detected at the bulging base of each canal (the ampulla). The vestibule (Ve) houses the utricle and the saccule, the two otolith organs of the ear that detect linear movements and accelerations, including gravity. Sounds are detected in the cochlea (Co), coiled around an axis. The sound waves are propagated through the oval window (OW); they propagate along the coils of the cochlea until its apex, then back to its base until they reach the round window (RW), where they dissipate. The vestibular aqueduct (VA) is connected to the vestibule, and is involved in hearing. Since it is made of soft tissue, the inner ear is not preserved in fossil specimens. However it is possible to study the bony labyrinth, its osseous surroundings in the thick petrous part of the temporal bone, because its shape roughly mimics the inner ear. Bony labyrinth anatomy has previously been demonstrated to provide phylogenetic, functional, and paleoecological signals.

In mammals, the semicircular canal morphology was found to be linked to agility (Spoor *et al*., 2007; Silcox *et al*., 2009; Perier *et al*., 2016; Gonzales *et al*., 2019; *contra* Morimoto *et al*., 2020), posture (Le Maître *et al*., 2017; Spoor & Zonneveld, 1998; Spoor *et al*., 1994, 1996), locomotion (Georgi, 2008; but see Rae *et al*., 2016), and ecology (Grohé *et al*., 2016; Pfaff *et al*., 2015; Ekdale, 2016; Schwab *et al*.,
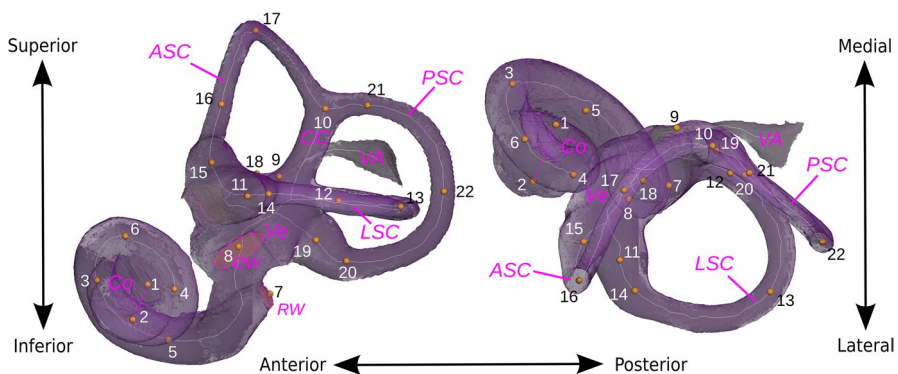

Fig. 1 Position of 22 landmarks on the left bony labyrinth of Macaca fascicularis MCZ-23812 in lateral (*left*) and superior (*right*) views. The landmarks are defined following Lebrun *et al*. (2010), as detailed in Appendix S2. *ASC*, anterior semicircular canal; *CC*, common crus; *Co*, cochlea; *LSC*, lateral semicircular canal; *OW*, oval window; *PSC*, posterior semicircular canal; *RW*, round window; *VA*, vestibular aqueduct; *Ve*, vestibule. The *dashed line* corresponds to the axis of the cochlea

2019). Recent studies have highlighted the importance of taking intraspecific variation into account in analyses of the adaptive signal, and not just the average morphology (Gonzales *et al*., 2019; Lebrun *et al*., 2021).

In primates, the morphology of the labyrinth is phylogenetically informative at high taxonomic levels (orders, infraorders, superfamilies, or families, see Lebrun *et al*., 2010, 2012; Morimoto *et al*., 2020). At lower taxonomic levels, genera, species, and subspecies can be discriminated in anthropoid primates based on labyrinth morphology, even if the exact pattern of phylogenetic relationships is not completely reflected (Spoor, 1993; Gunz *et al*., 2012; Beaudet *et al*., 2016; Urciuoli *et al*., 2020, Urciuoli & Zanolli, 2021; del Rio *et al*., 2021). Therefore, the bony labyrinth can be used to reconstruct the locomotor behavior of a fossil species or to assess its phylogenetic relationships with other taxa - at least at suprageneric taxonomic ranks, although discriminating between these two lines of evidence is not always straightforward.

The morphology of the labyrinth also reflects body dimensions. Heavier primates tend to have a larger bony labyrinth in absolute size, but smaller relative to their body mass (e.g., Spoor & Zonneveld, 1998; Spoor *et al*., 2007; Walker *et al*., 2008; Silcox *et al*., 2009; Ryan *et al*., 2012). A small but statistically significant fraction of the shape of the bony labyrinth is predicted by body mass (del Rio *et al*., 2021) or by labyrinth size (Le Maître *et al*., 2017; Urciuoli *et al*., 2020). Available evidence shows that in mammals, labyrinth size and shape change barely after petrous bone ossification, which happens before birth, at least in humans (Jeffery & Spoor, 2004; Mejdoubi *et al*., 2015, 2016; *contra* Boucherie *et al*., 2021) and ruminants (Maier, 2013; Mennecart & Costeur, 2016). Therefore, labyrinth morphological variation is likely to preclude size and shape variation involving biological mechanisms for which the onset occurs after the definitive size is acquired (e.g., allometric shape changes of the skull, sexual dimorphism). Because phylogeny, body mass, and ecology are not totally independent in primates, disentangling these three elements in labyrinth morphology is even more difficult.

In the present study, we attempt to clarify the phylogenetic affinities of the fossil genus *Paradolochopithecus*, based on the bony labyrinth of the cranium LGPUT DFN3-150 of *Paradolichopithecus* aff. *arvernensis* from the Lower Pleistocene site of Dafnero-3 in Northwestern Greece, identified as a subadult female (Kostopoulos *et al*., 2018). For this purpose, we analyse the morphology of this structure, reconstructed from micro-CT scan imaging, using geometric morphometric methods. We investigate the potential of bony labyrinth morphology to reconstruct phylogenetic relationships within Cercopithecinae, and we assess the impact of allometry on labyrinth shape. Based on these elements, we use the bony labyrinth to clarify the affinities of the fossil with Macacina and Papionina, the two extant subtribes of the cercopithecine tribe Papionini.

As body mass is highly variable across Cercopithecinae, we anticipate that size is the main component of morphological variation for the bony labyrinth (hypothesis H1), so we predict a larger labyrinth for larger primates (prediction P1). Because allometry is known to be an important component of skull shape variation in this group (Frost *et al*., 2003; Joganic & Heuzé, 2019; Joganic *et al*., 2018; Nishimura *et al*., 2019; Profico *et al*., 2017), we propose the hypothesis that this

also applies to the inner ear (H2). Therefore, we predict that the main component of shape variation is allometry (P2). If the first hypothesis (H1) is supported, then we predict that because of its heavy body mass (ca. 19.5 kg; Kostopoulos *et al.*, 2018), the bony labyrinth of the fossil specimen of *Paradolichopithecus* would be large and, together with H2, it would imply a shape similar to that of large Papionina. Based on previous studies in related primates, we propose the hypothesis that the labyrinth morphology of Cercopithecinae reflects both phylogeny and ecology (H3). We do not specifically test the adaptive signal in the present study, but we can predict from H3 that we will find a phylogenetic signal in labyrinth morphology (P3a), and that because it is blurred by the adaptive signal, labyrinth morphology better reflects phylogeny at high taxonomic levels (P3b). However, as body mass in Papionina tends to be larger than in Macacina and Cercopithecini, we suppose that the phylogenetic signal in the bony labyrinth morphology is mainly driven by size (H4), which predicts a weaker signal when size effects are removed (P4). If the two hypotheses regarding the phylogenetic signal (H3 and H4) are true, then we can use the labyrinth morphology as an indicator of the phylogenetic affinities of the fossil. However, if H2 is true, we should preferentially remove the allometric component of shape, to avoid size effects.

Methods

Sample Composition

The fossil cranium LGPUT DFN3-150 of *Paradolichopithecus aff. arvernensis* is housed in the Museum of Geology–Palaeontology–Palaeoanthropology of the Aristotle University of Thessaloniki (LGPUT). We collected high-resolution micro-computed tomography (HR-µCT) images at the PLATeforme INstrumentale d'Analyses – PLATINA (IC2MP, Université de Poitiers). The protocol followed and the technical parameters are given in Appendix S1 and by Kostopoulos *et al.* (2018).

The comparative sample for the morphometric study of the labyrinth (Table I; Appendix S1: table) consisted of µCT-scans of the dry skulls of 80 specimens representing 25 extant species in ten cercopithecine genera. Because *Paradolichopithecus* is thought to be a Papionini, we mainly included specimens from this tribe: 35 Papionina (six specimens of *Cercocebus*, six *Lophocebus*, eight *Mandrillus*, ten *Papio*, five *Theropithecus*) and 32 Macacina (genus *Macaca*). For comparisons, we added 13 specimens representing four genera of Cercopithecini (one *Allochrocebus*, two *Cercopithecus*, seven *Chlorocebus*, and three *Erythrocebus*). Thirty-four specimens are females, 39 specimens are males, while the sex was not available for the rest of the sample. Twenty-five individuals are juveniles or young adults (as their third molars are not fully erupted), but they can be included in the comparison, since maturity does not affect the labyrinthine morphology (Jeffery & Spoor, 2004).

Species	Sex[a]			Total
	F	M	NA	
Fossil (*n*=1)				
Paradolichopithecus aff. *arvernensis*	1	0	0	**1**
Cercopithecini (*n*=13)				
Allochrocebus lhoesti	0	1	0	**1**
Cercopithecus cephus	1	1	0	**2**
Chlorocebus aethiops	1	2	1	**4**
Chlorocebus pygerythrus	2	1	0	**3**
Erythrocebus patas	1	2	0	**3**
Papionina (*n*=35)				
Cercocebus agilis	2	1	0	**3**
Cercocebus atys	0	1	0	**1**
Cercocebus torquatus	1	1	0	**2**
Lophocebus albigena	4	2	0	**6**
Mandrillus leucophaeus	1	3	2	**6**
Mandrillus sphinx	0	2	0	**2**
Papio anubis	5	1	0	**7**
Papio cynocephalus	1	1	0	**2**
Papio hamadryas	0	1	0	**1**
Theropithecus gelada	2	3	0	**5**
Macacina (*n*=32)				
Macaca fascicularis	6	3	2	**11**
Macaca fuscata	2	0	1	**3**
Macaca hecki	2	0	0	**2**
Macaca leonina	1	0	0	**1**
Macaca maura	0	1	0	**1**
Macaca mulatta	2	2	0	**4**
Macaca nigra	1	0	0	**1**
Macaca radiata	1	0	0	**1**
Macaca sp.	0	1	0	**1**
Macaca sylvanus	1	4	0	**5**
Macaca thibetana	1	0	1	**2**

Table I Summary of the sample used for the study of the bony labyrinth of the fossil specimen, compared to extant species (*n*=80). Papionina and Macacina are two subtribes of tribe Papionini, the sister group of the tribe Cercopithecini. See appendix S1 for more details

[a] Sex: F, female; M, male; NA, not available

Data Acquisition

We downloaded the microCT-scans of 37 primate skulls from the MorphoSource website (www.MorphoSource.org, Duke University), which have resolutions ranging from 58.7 to 123.3 μm (isometric voxel size). We also scanned 15 skulls using an X-ray microtomograph at the IC2MP, Université de Poitiers, at resolutions ranging from 13.0 to 74.0 μm (isometric voxel size): six specimens are curated by the Royal Museum of Central Africa, Tervuren, Belgium, one by PALEVOPRIM lab,

and eight by the Muséum National d'Histoire Naturelle, Paris, France. Finally, we directly used the 3D surface of the bony labyrinth for 28 specimens from three different museums, which were scanned at resolutions ranging from 33 to 96 μm (isometric voxel size), and virtually extracted by Beaudet *et al*., (2016, 2019; personal communication; see Appendix S1 for more details).

We virtually extracted the bony labyrinth on one side (preferentially left) from the microCT-scans using Amira (Thermo Fisher Scientific) software, and processed the generated surfaces using GeomagicStudio (Geomagic, Inc.) software to remove artifacts (little holes and spikes, overlapping mesh triangles). After calculating the centerline of the 3D volume (using the 'auto skeleton' tool in Amira), we positioned 22 landmarks on the surface and the centerline of the labyrinth (Lebrun *et al*., 2010; Le Maître, 2019; Fig. 1; see Appendix S2 for landmark definitions, and Appendix S3 for raw landmark coordinates). When we extracted the right labyrinth, we mirrored the surface using GeomagicStudio software for comparisons with the left side. For the fossil specimen, we extracted both left and right sides (Appendix S4-1 and S4-2).

Analyses

Allometry

Using R v4.1.1 software (R Development Core Team, 2021), we aligned, rotated, and scaled the 3D landmark coordinates by a Procrustes superimposition (Bookstein, 1991; Rohlf & Slice, 1990). To assess the effect of body mass on labyrinth size, we did an ordinary least squares (OLS) regression of labyrinth centroid size on body mass, in log scale. We also tested the effect of body mass on labyrinth shape using a multivariate regression of the Procrustes shape coordinates on the natural logarithm of body mass. Because we found an association between body mass and labyrinth centroid size, we also tested the joint effect of body mass and centroid size on labyrinth shape, using a regression of the Procrustes shape coordinates on both variables expressed in log scale, with and without interaction effects. We conducted all analyses on the 79 extant specimens (without the fossil and the undefined *Macaca*). As body mass was not available for each individual, we used for each species the arithmetic mean body mass for a male or a female (Delson *et al*., 2000). When the sex was not determined, we excluded the observation.

To quantify the allometric effects within the bony labyrinth, we performed a multivariate regression of the Procrustes shape coordinates on the natural logarithm of centroid size (Bookstein, 1991; Mitteroecker *et al*., 2013), using an ordinary least squares estimation method. We performed a permutation test with 10,000 iterations against the null hypothesis of independence between the size and shape variables. We visualised the regression score as a function of log centroid size (CS). The regression score corresponds to the shape variable that is most strongly associated with the independent variable, here log CS ("shape score [defined] by projecting the shape data onto a line in the direction of the regression vector for the independent variable"; Drake & Klingenberg, 2008). As it has been argued that *Paradolichopithecus* might be a large macaque (Delson & Frost, 2004; Strasser & Delson, 1987),

we visualised the line corresponding to the ordinary least squares regression of the regression score on log centroid size for the whole sample, and for three clades: Cercopithecini, Papionina, and Macacina (the two latter representing together the extant Papionini subtribes). We used the same clades to compute the bgPCA (see below). From this, we could see the regression score predicted for a primate having the same CS as the fossil LGPUT DFN3-150, to check whether its morphological similarities with baboons might be due to allometry. The prediction is much less reliable for the regression based on Macacina compared to Papionina (and Cercopithecini), because the former is an extrapolation (estimation beyond the observation range for Macacina), whereas the latter is an interpolation (estimation within the observation range for Papionina and Cercopithecini).

Morphological Variation

To explore the morphological diversity of the inner ear across cercopithecines, we performed a principal component analysis (PCA) on all specimens. We used the Procrustes shape coordinates as variables. To check whether any principal component corresponds to the allometric signal, we assessed the strength of the association between each PC and centroid size. For comparison, we also conducted a PCA on the residuals of the regression of Procrustes shape coordinates on log centroid size. As the results were very similar for both principal component analyses, we only present the results for Procrustes shape coordinates in the main text, and we used these variables for all further analyses. We performed all analyses using the *MASS* (Venables & Ripley, 2002), *geomorph* 4.0.3 (Adams *et al.*, 2021; Baken *et al.*, 2021) and *Morpho* 2.9 (Schlager, 2017) packages in R, and visualised the 3D shape changes associated with the principal components as warped surfaces using the *rgl* 0.106.8 (Murdoch & Adler, 2021) and *Morpho* packages.

To get a better separation among the three clades (Cercopithecini, Papionina, and Macacina), we performed a between-group principal component analysis (bgPCA). We preferred this type of analysis, rather than a canonical variate analysis, because the conditions of multivariate normality and homoscedasticity are unlikely to be met (Boulesteix, 2005; Mitteroecker & Bookstein, 2011). As the number of morphological variables is high relative to the number of cases per group, we conducted the analyses on reduced data to avoid spurious group discrimination (see Bookstein, 2019; Cardini & Polly, 2020 for caution on bgPCA): the first seven principal components (53.4% of the explained variance) obtained from the PCA based on the Procrustes shape coordinates. The number of principal components corresponds to the minimum number of PCs required to get the best classification rate. We performed a leave-one-out cross-validation to test the robustness of the prediction. We projected the position of the fossil in the morphological space of the between-group principal components (bgPCs). We also computed the typicality probabilities for the fossil to belong to each clade, based on the bgPCs. For the computation of typicality probabilities, we adjusted Mahalanobis D^2 for small sample sizes as suggested by Wilson (1981). We performed the analyses using the functions "groupPCA", "predict.bgPCA", and "typprobClass" of the package *Morpho* (Schlager, 2017).

Phylogenetic Signal

Using the "nj" function of the package *ape* 5.0 (Paradis & Schliep, 2019), we performed neighbor-joining clustering analyses based on the Euclidean distances among Cercopithecinae species (Saitou & Nei, 1987). We computed the Euclidean distances based on form (Procrustes shape coordinates and log CS), shape (Procrustes shape coordinates), and allometry-free shape (regression residuals). The Euclidean distances between Procrustes shape coordinates correspond to Procrustes distances.

We tested the phylogenetic signal using the *K*-statistic (Blomberg *et al*., 2003) and its multivariate version the K_{mult} statistic (Adams, 2014), on the mean labyrinth morphology of each extant species, for the whole sample and for Papionini only (we excluded the *Macaca* specimen without species identification). We tested the signal for centroid size (= size), for regression residuals (= allometry-free shape), for Procrustes shape coordinates (= shape), and for Procrustes shape coordinates and log centroid size (= form). When $K > 1$, the phylogenetic signal is greater than what is expected under a Brownian motion model (i.e., variance is greater among clades), and lower if $K < 1$ (i.e., variance is greater within clades). $K = 1$ corresponds to a morphology that follows a Brownian motion model (i.e., perfect drift). We performed permutations of the shape data among the tips of the phylogeny with 1,000 iterations, to test for statistical significance against the null hypothesis of no pattern of similarity among relatives (i.e., no phylogenetic signal). We conducted the evaluation of the phylogenetic signal using the "physignal" function of the *geomorph* package (Adams *et al*., 2021; Baken *et al*., 2021). The reference tree (Appendix S5) was the consensus chronogram tree (branch length proportional to absolute time) for the Bayesian phylogeny of the 25 modern species, based on the GenBank dataset and downloaded from the version 2 of 10kTrees website (Arnold *et al*., 2010; https://10ktrees.nunn-lab.org/index.html).

Ethical note

The fossil specimen was found during paleontological excavations in Greece. We conducted the excavations according to local regulations, with due authorization from all relevant parties. All primates included in the comparative sample were dry skulls from historical collections housed in public museums or universities. Therefore, our study did not imply specific issues regarding animal welfare. For all specimens, we had the relevant authorization (depending on the kind of data; see below) to perform microCT-scanning, to use microCT-scans for the virtual extraction, and/or to use 3D mesh surfaces of the labyrinth. The authors declare no conflict of interest.

Data availability All data generated or analysed during this study are included in this published article and its supplementary information files.

Results

Comparative anatomy

Because of sediment filling, the reconstruction of the right labyrinth of the fossil LGPUT DFN3-150 is much more rugged than the left one, and little parts of the basal turn of the cochlea are missing (Fig. 2, Appendix S4-1 and S4-2). Compared to the left side, it is slightly distorted, with a somewhat flattened basal turn of the cochlea, and a slight elongation along the anteromedial–posterolateral axis. The left labyrinth is not distorted.

Paradolichopithecus labyrinth morphology does not exactly match that of any extant species, but it is most similar to *Erythrocebus patas*, a Cercopithecini, and *Mandrillus leucophaeus*, a Papionina (Fig. 2). It shares with both Cercopithecini and Papionina i) a cochlea with more than three turns, and ii) a superior projection of the anterior and posterior semicircular canals (ASC and PSC, respectively) relative to the common crus, even if the latter canal is relatively less projected in Papionina because of their longer common crus. The specimen LGPUT DFN3-150 also shares with Papionina a posterolaterally projected lateral semicircular canal (LSC), even when taking into account the potential distortion of the fossil. However, some similarities can also be found with Macacina, such as the more laterally facing cochlea, and the branching of the posterior part of the LSC on the vestibule that is more superior relative to the PSC (a feature also observed in some Cercopithecini). Finally, some features are specific to *Paradolichopithecus* labyrinth, such as its unique torsion pattern for the PSC.

Size variation and allometry

When only extant species are considered ($n = 71$, excluding *Macaca* sp. and observations with undetermined sex), there is a statistically significant positive correlation between labyrinth centroid size and body mass ($R^2 = 0.4765$; $F_{1,69} = 62.8$; $p < 0.005$). Procrustes shape coordinates are also significantly associated with body mass ($R^2 = 0.0272$; $F_{1,69} = 1.9287$; $p = 0.0078$). When the additive effect of body mass and labyrinth centroid size is evaluated, we find a significant association of both variables with Procrustes shape coordinates ($p = 0.0067$ for body mass and $p = 0.0033$ for centroid size). For a model with an interaction term between body mass and labyrinth centroid size, we still find significant associations with shape coordinates ($p = 0.0062$ and $p = 0.0028$, respectively), with a significant interaction effect ($p = 0.0169$).

Papionina tend to have a larger bony labyrinth than the other Cercopithecinae, especially *Papio anubis* (Fig. 3). In contrast, Cercopithecini have a small labyrinth, except for the two *Erythrocebus* male specimens. For labyrinth size, Macacina overlap with Cercopithecini. They also completely overlap with the
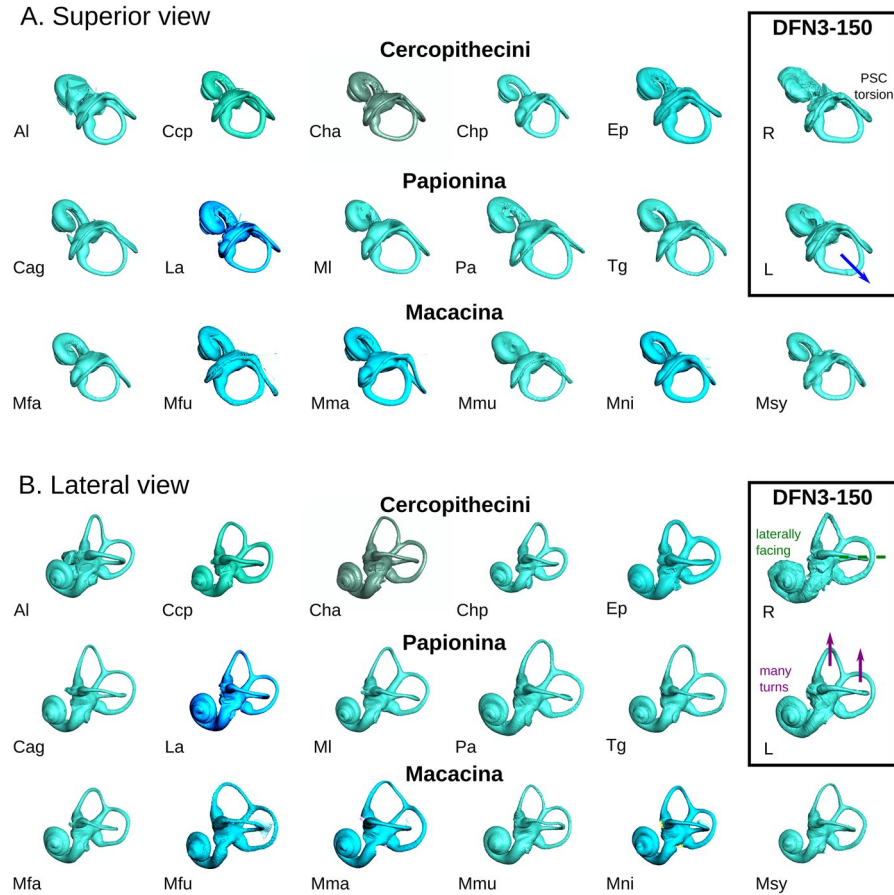
Fig. 2 Bony labyrinth of extant species, compared to the two labyrinth (*R*, right; *L*, left) of the fossil specimen *Paradolichopithecus aff. arvernensis* LGPUT DFN3-150. The bony labyrinth is visualised as from the left side (right side mirrored), in orthographic view. The anatomical features that the fossil shares with both Cercopithecini and Papionina (cochlea with many turns, superior projection of the ASC and PSC relative to the common crus) are highlighted in *purple*, with Papionina only (posterolateral projection of the LSC) in *blue*, and with Macacina (laterally facing cochlea, superior branching of the LSC) in *green*. The torsion pattern of the PSC is unique to the fossil taxon. **a** Superior view. **b** Lateral view. (*Top*) Cercopithecini: *Al*, *Allochrocebus lhoesti* (83–006-M153); *Ccp*, *Cercopithecus cephus* (MHNT-OST-AC-515); *Cha*, *Chlorocebus aethiops* (MHNT-OST-AC-523); *Chp*, *Chlorocebus pygerythrus* (MNHN-1972–302); *Ep*, *Erythrocebus patas* (MRAC-8452). (*Middle*) Papionina: *Cag*, *Cercocebus agilis* (AMNH-M-52635); *La*, *Lophocebus albigena* (MRAC-37572); *Ml*, *Mandrillus leucophaeus* (MNHN-2002–105); *Pa*, *Papio anubis* (AMNH-M-52668); *Tg*, *Theropithecus gelada* (MNHN-1969–449. (*Bottom*) Macacina: *Mfa*, *Macaca fascicularis* (MCZ-12758); *Mfu*, *Macaca fuscata* (AMNH-M-35640); *Mma*, *Macaca maura* (AMNH-M-90159); *Mmu*, *Macaca mulatta* (MCZ-61414); *Mni*, *Macaca nigra* (AMNH-M-196409); *Msy*, *Macaca sylvanus* (NMHN-M-476780)

smallest Papionina (*Lophocebus*, *Theropithecus* and *Cerocebus*) and partially with larger Papionina (*Mandrillus* and *Papio*), except *Macaca fascicularis* and *M. nigra*, which have a smaller labyrinth.
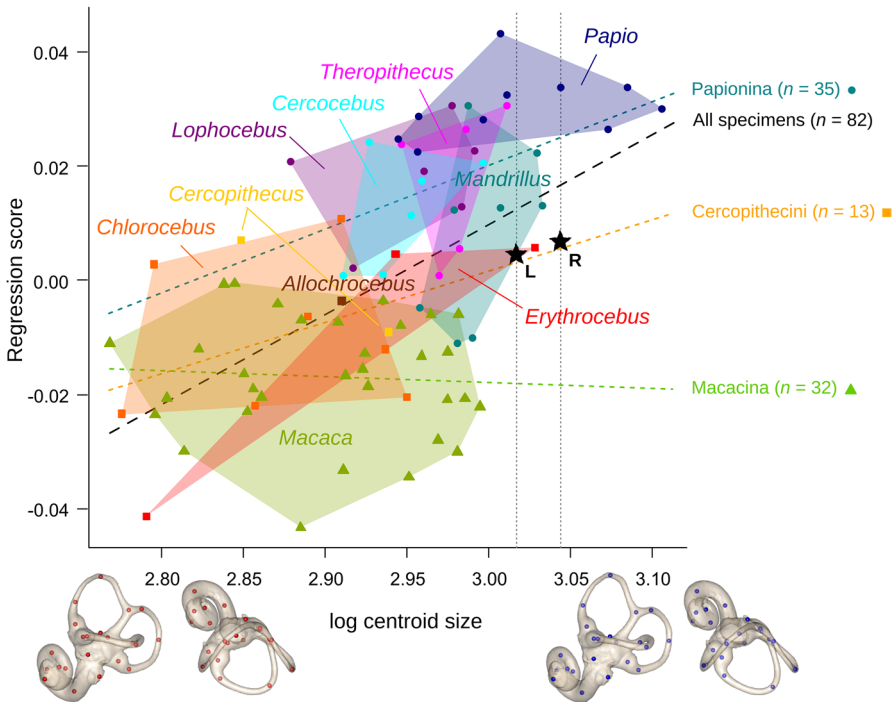
Fig. 3 Allometric trend for the labyrinth in Cercopithecinae. The labyrinth centroid sizes (in mm) are shown in logarithmic scale. The fossil specimen LGPUT DFN3-150 is represented by *stars* for the left (*L*) and right (*R*) sides. The *squares* correspond to Cercopithecini, the *circles* correspond to Papionina, and the *triangles* correspond to Macacina. *Convex hulls* delineate genera. The predicted shape configurations at minimum and maximum sizes are represented as warped surfaces (orthographic projections of the left surface – *left*, lateral view; *right*, superior view). The regression lines of the regression score on log centroid size are plotted for the whole sample (*black line*) and for the different clades: Cercopithecini (*orange*), Papionina (*turquoise*) and Macacina (*green*). The *vertical lines* correspond to centroid size for each side of the fossil LGPUT DFN3-150

Size has a significant effect on shape for the bony labyrinth, but the association is weak ($n = 82$, $F_{1,80} = 1.828$, multiple $R^2 = 0.021$, $p < 0.001$). Compared to Macacina, all Papionina have i) a larger, more superiorly projected, and less twisted ASC, ii) a LSC which is more twisted, more posterolaterally projected and less anteriorly projected, and iii) a more twisted and coiled first cochlear turn (Fig. 3). Only three *Mandrillus leucophaeus* (female or unidentified sex) share some shape similarities with some macaques. Cercopithecini have intermediate shapes between Macacina and Papionina, with more similarities to the former,

Fig. 4 Four first principal components of the Procrustes shape coordinates of the bony labyrinth in Cercopithecinae. **a** PC2 vs PC1. **b** PC3 vs PC1. **c** PC4 vs PC1. See legend of Fig. 3 for a detailed description of symbols ▶
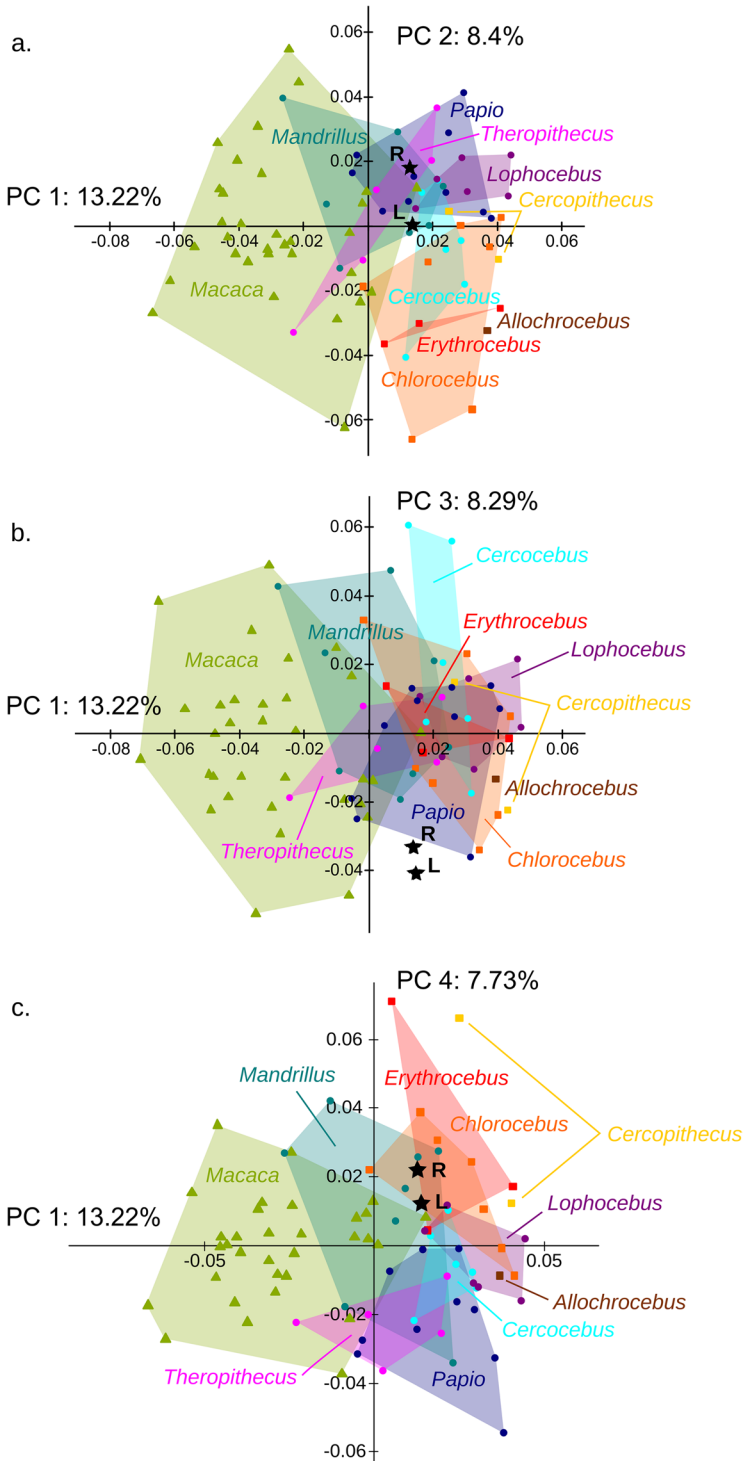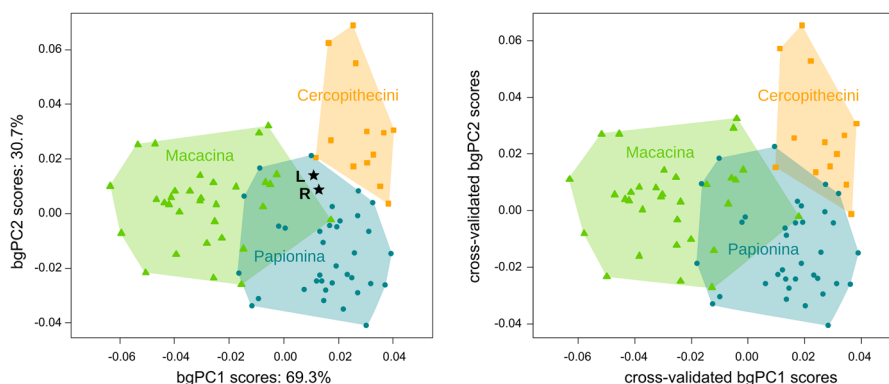
Fig. 5 Between-group principal components (bgPC) of seven shape variables describing the bony labyrinth of extant cercopithecines. The shape variables were the first seven principal components of Procrustes shape coordinates. Convex hulls enclose each group used for the classification, and the black stars corresponds to the projection of the left (*L*) and right (*R*) labyrinths of the fossil LGPUT DFN3-150 on the space of bgPC1 and bgPC2. The *left panel* represents the scores for bgPC2 (30.7% of the between-group variance explained) vs bgPC1 (69.3% of the between-group variance explained). The *right panel* represents the cross-validated scores

especially for one female *Erythrocebus patas* having extreme *Macaca*-like features. The fossil specimen (LGPUT DFN3-150; a female specimen; Kostopoulos *et al.*, 2018) is characterized by high CS values, similar to *Papio*, *Theropithecus*, *Mandrillus*, and male *Erythrocebus patas*, and it has an intermediate shape, like Cercopithecini, but closer to Papionina (Fig. 3; Appendix S6: Fig. 2).

The regression lines for Cercopithecini and Papionina are roughly parallel, and their slopes have the same sign as the overall regression line (slope = 0.16), but unlike the regression slope for Macacina (Fig. 3; Appendix S6: Fig. 1). The fossil LGPUT DFN3-150 is positioned on the Cercopithecini line and close to the overall regression line, but far below the Papionina line (but three *Mandrillus* are further away), and clearly above the Macacina line beyond the 90% prediction band (Appendix S6: Fig. 1).

Shape variation

Although with considerable overlap, the first four principal components of the Procrustes shape coordinates (37.6% of the total variance; see Appendix S7: Fig. 1) separate three groups: Cercopithecini, Papionina, and Macacina (Fig. 4; Appendix S7: Figs. 2, 3; Appendix S8). Despite considerable overlap, especially for *M. fascicularis*, the first principal component (PC1; 13.2% of the total variance) tends to separate Macacina (lower scores) from the two other groups, whereas the second principal component (PC2; 8.4% of the total variance) distinguishes Cercopithecini (lower scores) from Papionina. Papionina overlap with both groups. *Mandrillus*, *Theropithecus* and *Papio* overlap with Macacina along PC1, while *Cercocebus* and *Theropithecus* overlap with Cercopithecini along PC2. There is no clear trend along
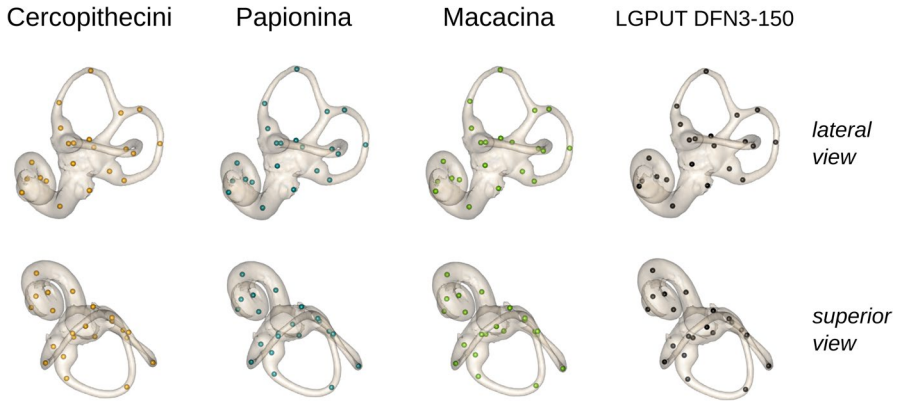
| Cercopithecini | Papionina | Macacina | LGPUT DFN3-150 | |

Cercopithecini Papionina Macacina LGPUT DFN3-150

lateral view

superior view

Fig. 6 Shape configuration (average of left and right sides) of the fossil LGUT DFN3-150, compared to the average shape configurations of Cercopithecini, Papionina, and Macacina (orthographic projections of the left surface —*top*, lateral view; *bottom*, superior view). The average shape configurations are warped surfaces obtained from the deformation of the surface of a reference specimen (specimen *Theropithecus gelada* MNHN-ZM-MO-1972-360), based on Procrustes shape coordinates

the third principal component (PC3; 8.3% of the total variance), except a separation between the two *Cercocebus torquatus* (high scores) and the other *Cercocebus* species and, within Papionina, a distinction between the genera *Cercocebus* and *Mandrillus* (higher scores) on one end and the other papionin genera on the other end. The fourth principal component (PC4; 7.7% of the total variance) partially separates Cercopithecini (higher scores) from certain Papionina (*Theropithecus*, *Papio*). Considering together the four first principal components, the fossil specimen has no clear affinities with any clade, but it slightly tends to group with Papionina, very close to both *Papio* and *Mandrillus* (Fig. 4; Appendix S7: Figs. 2, 3; Appendix S8).

The shape variation associated with each principal component corresponds to changes in both the cochlea and the semicircular canal system. These shape changes are different from allometric shape changes, except some similarities for PC4 such as the posterolateral projection of the LSC and the superior projection of the ASC (for a detailed description of the shape variation patterns, see Appendix S7: Fig. 4). The fossil specimen has positive PC1 scores because of the posterolateral projection of the LSC and the superior projection of the vertical semicircular canals (relative to the short common crus), a condition shared with Papionina. Its slightly positive PC2 scores are related to the laterally facing cochlea. Its strongly negative PC3 scores correspond to a less round LSC, an increased torsion of the PSC, and more superoinferiorly projected vertical semicircular canals. Finally, its slightly positive PC4 scores are due to the inferior projection of the PSC relative to the LSC.

The association between each principal component and centroid size is very weak for PC1, PC2, and PC4, and completely negligible for PC3 (correlation coefficients as low as PC1 0.21, PC2 0.15, PC3 0.02, and PC4 − 0.23). Therefore, it is not surprising to find a very similar distribution of the species for the PCA on Procrustes shape coordinates (described above and in Appendices S7 and S8) and for the PCA on the residuals of their regression on log centroid size (Appendix S9: Figs. 1 and 2).

Table II Typicality probabilities for the fossil LGPUT DFN3-150 to belong to each clade, based on the bgPCs. Probabilities are given separately for the left and right sides, with the highest probability in bold
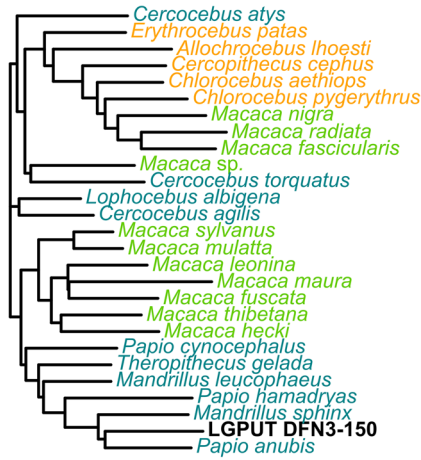
	Cercopithecini	Macacina	Papionina
Left	**0.323**	0.043	0.211
Right	0.248	0.040	**0.354**

For the bgPCA conducted on the first seven PCs of the Procrustes shape variables, the classification success is good, with 86.25% correct classification for the leave-one-out cross-validation (91.25% without cross-validation). With the leave-one-out cross-validation, six Papionina (8.6%) were misclassified as Macacina (three) and as Cercopithecini (three); four Macacina (12.5%) were misclassified as Papionina (two) or Cercopithecini (two); and only one Cercopithecini (7.7%) was misclassified as Papionina. There is a strict separation between Cercopithecini and Macacina along the first between-group principal component (69.3% of the explained variance between groups) and, when both bgPCs are considered, Papionina occupy an intermediate position that partially overlaps with Macacina, especially *M. fascicularis*, while being separated from Cercopithecini (Fig. 5a; Appendix S10). The bgPC scores are very similar to their cross-validated counterparts, except a limited overlap between Papionina and Cercopithecini for cross-validated scores, which means that there is no spurious group separation (Fig. 5b; Appendix S10). The fossil LGPUT DFN3-150 is located within the shape distribution of Papionina. It is outside the shape distribution of both Macacina and Cercopithecini when the two bgPCs are taken into account, but it remains close to the border of the convex hulls of both clades. Typicality probabilities do not return a clear grouping for the fossil LGPUT DFN3-150, except that it is not a Macacina. Whereas the left labyrinth is classified as a Cercopithecini, the right side is classified as a Papionina (Table II).
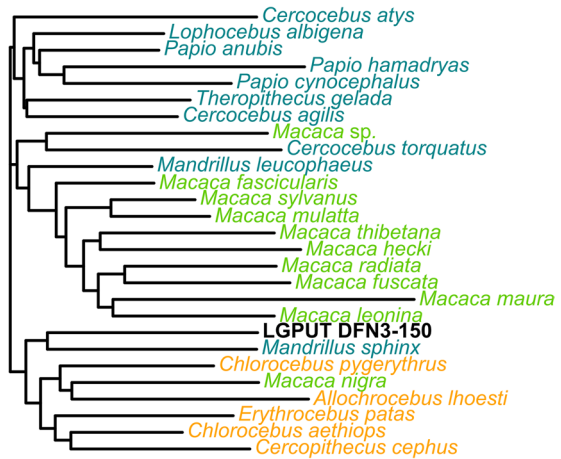
Compared to the average shape configuration of the three extant clades (Fig. 6), the bony labyrinth of *Paradolichopithecus* aff. *arvernesis* is elongated in the antero-medial–posterolateral axis, with smaller and less round semicircular canals, a LSC that branches more superiorly on the common crus, and a more horizontal cochlear axis. The posterolateral projection of the LSC is common between *Paradolichopithecus* and the average Papionina. Relative to the average Papionina and Cercopithecini, the fossil shares some similarities with the average Macacina, such as a short common crus, a less twisted LSC, and a less superiorly projected ASC. However, contrary to *Paradolichopithecus*, the common crus is shifted superiorly and the superior part of the PSC is projected anteriorly in the average Macacina.

Fig. 7 Dendrograms resulting from NJ cluster analyses based on the Euclidean distances among species ▶ computed for (**a**) Procrustes shape coordinates and log centroid size; (**b**) Procrustes shape coordinates; (**c**) Residuals from the regression of Procrustes shape coordinates on log centroid size. *Orange*, Cercopithecini; *green*, Macacina; *turquoise*, Papionina
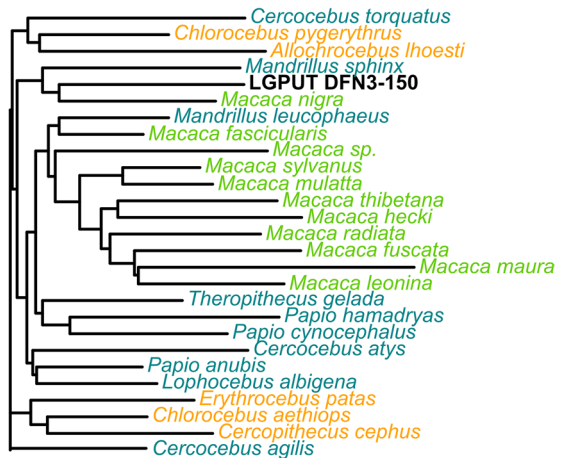
a. Procrustes coordinates
and log centroid size

Cercocebus atys
Erythrocebus patas
Allochrocebus lhoesti
Cercopithecus cephus
Chlorocebus aethiops
Chlorocebus pygerythrus
Macaca nigra
Macaca radiata
Macaca fascicularis
Macaca sp.
Cercocebus torquatus
Lophocebus albigena
Cercocebus agilis
Macaca sylvanus
Macaca mulatta
Macaca leonina
Macaca maura
Macaca fuscata
Macaca thibetana
Macaca hecki
Papio cynocephalus
Theropithecus gelada
Mandrillus leucophaeus
Papio hamadryas
Mandrillus sphinx
LGPUT DFN3-150
Papio anubis

b. Procrustes coordinates

Cercocebus atys
Lophocebus albigena
Papio anubis
Papio hamadryas
Papio cynocephalus
Theropithecus gelada
Cercocebus agilis
Macaca sp.
Cercocebus torquatus
Mandrillus leucophaeus
Macaca fascicularis
Macaca sylvanus
Macaca mulatta
Macaca thibetana
Macaca hecki
Macaca radiata
Macaca fuscata
Macaca maura
Macaca leonina
LGPUT DFN3-150
Mandrillus sphinx
Chlorocebus pygerythrus
Macaca nigra
Allochrocebus lhoesti
Erythrocebus patas
Chlorocebus aethiops
Cercopithecus cephus

c. Regression residuals

Cercocebus torquatus
Chlorocebus pygerythrus
Allochrocebus lhoesti
Mandrillus sphinx
LGPUT DFN3-150
Macaca nigra
Mandrillus leucophaeus
Macaca fascicularis
Macaca sp.
Macaca sylvanus
Macaca mulatta
Macaca thibetana
Macaca hecki
Macaca radiata
Macaca fuscata
Macaca maura
Macaca leonina
Theropithecus gelada
Papio hamadryas
Papio cynocephalus
Cercocebus atys
Papio anubis
Lophocebus albigena
Erythrocebus patas
Chlorocebus aethiops
Cercopithecus cephus
Cercocebus agilis

Clustering analyses

Dendrograms reconstructed from neighbour-joining clustering algorithm differ depending on the way size variation is included. When log centroid size is included, the larger Papionina (*Papio*, *Theropithecus*, *Mandrillus*) cluster together, and the fossil falls within this group, closest to *Papio anubis* and *Mandrillus sphinx* (Fig. 7a). A cluster of seven larger *Macaca* forms the nearest group of the cluster of larger Papionina. All Cercopithecini cluster together, with a group of three small *Macaca* species branching inside. The smaller Papionina (*Cercocebus*, *Lophocebus*) branch more basally relative to these clusters. Labyrinth centroid size is clearly the main driver of the clusterings in this case.

For the analysis based on Procrustes shape coordinates only, all Macacina cluster together, except for a *Macaca* sp. and the *M. nigra* specimen (Fig. 7b). The latter falls inside another cluster made by all Cercopithecini. Most Papionina cluster together, except *Cercocebus torquatus* and the two species of *Mandrillus*. *Mandrillus sphinx* with the fossil taxon forms the nearest group of Cercopithecini, whereas *Mandrillus leucophaeus* and *Cercocebus torquatus* cluster with the Macacina group.

7The analysis based on regression residuals shows many similarities with the analysis based on Procrustes shape coordinates with regard to the Macacina cluster (Fig. 7c). However, Papionina and Cercopithecini are mixed in several small clades that all branch basally relative to Macacina. As in other clustering analyses, the fossil taxon groups with *Mandrillus sphinx*, together with *Macaca nigra*, but outside the Macacina cluster. For all analyses, the pattern of clustering within each subtribe (Cercopithecini, Macacina and Papionina) is not consistent with the molecular phylogeny (Fig. 7a–c).

Phylogenetic signal

When all extant cercopithecines are considered, we get a weak phylogenetic signal ($0.3 < K_{mult} < 0.4$), with closely related taxa having less similar morphologies than the expectation under a Brownian motion model: shape and size variance is larger within clades than among clades (Table III). The phylogenetic signal is slightly weaker in centroid size, compared to Procrustes shape coordinates or regression residuals. We

Table III Phylogenetic signal in the morphology of the bony labyrinth for extant Cercopithecinae and for the tribe Papionini. The star (*) indicates a statistically significant signal *(p < 0.05)*

	Cercopithecinae		Papionini	
	K or K_{mult}	P	K or K_{mult}	P
Centroid size	0.324	0.382	0.308	0.538
Regression residuals	0.369	0.005*	0.369	0.044*
Procrustes shape coordinates	0.380	0.001*	0.383	0.013*
Procrustes shape coordinates & log centroid size	0.362	0.024*	0.356	0.143

get very similar results when the analyses are conducted for extant Papionini only (Table III). *P*-values are below the 5% threshold as long as Procrustes shape coordinates are taken into account (except for Papionini when log centroid size is considered together with the coordinates), but not for centroid size alone. However, interpreting these results is tricky, because the null hypothesis of no pattern of similarity among relatives is very unlikely to be true in any biological organism.

Discussion

Our results show a very large variation in labyrinth centroid size in extant Cercopithecinae, with a larger labyrinth for heavier primates, which means that size is an important component of morphological variation (supports H1; Table IV). However, despite some association between labyrinth shape and size, allometry is only a very small component of shape variation (*contra* H2; Table IV). Clustering analyses show that labyrinth morphology reflects phylogeny at the tribe and the subtribe levels (supports H3), but not the fine pattern at lower taxonomic levels (*contra* H3; Table IV). The latter result might be explained by the superimposition of an adaptive signal (supports H3). Centroid size alone does not bear a phylogenetic signal, and the removal of allometric change only slightly weakens the signal in labyrinth shape, which means that size might partially drive the phylogenetic signal, but only indirectly, through minor allometric shape changes (*contra* H4; Table IV).

Because allometry partially drives the phylogenetic signal in labyrinth shape variation in Cercopithecinae, without being its main component, we should not regress out the size component to infer the affinities of the fossil specimen. As predicted for *Paradolichopithecus*, we found a large bony labyrinth, and many shape similarities with the large Papionina, even if it also has some affinities with other cercopithecines, especially Cercopithecini. Our findings on the bony labyrinth morphology do not support closest relationships with Macacina. However, it is difficult to decide whether *Paradolichopithecus* was a Papionina retaining some ancestral traits common to most Cercopithecinae, or a stem Papionini with closer affinities with Papionina.

As has been stressed by previous authors (e.g., Jablonski, 2002; Szalay & Delson, 1979) *Procynocephalus* and *Paradolichopithecus* show a mixture of outer cranial morphometric features between the mostly African *Papio* and the predominantly Eurasian *Macaca* (both extant taxa used in these studies as proxies of the morphological and phylogenetic divergences between the two main lineages of Papionini). Several studies (e.g., Jablonski, 2002; Nishimura *et al*., 2014; O'Shea *et al*., 2016; Rae, 2008; Szalay & Delson, 1979; Takai *et al*., 2008) suggest that external cranial morphology and inner nasal architecture of *Paradolichopithecus* exclude it from Papionina and place it closer to the crown lineage of *Macaca*. Resonant exceptions are the studies of Maschenko (1994, 2005), who directly refers *Paradolichopithecus* from Kuruksay (Tajikistan) to the genus *Papio*. Similarly to outer cranial features, the bony labyrinth of *Paradolichopithecus* shares anatomical features with both Macacina and Papionina. Some characters shared with Papionina might be plesiomorphic, like the superior projection of the vertical semicircular canals and the high

number of turns of the cochlea, which are also found in Cercopithecini. However, the overall anatomy of the bony labyrinth points to more affinities with Papionina, particularly with the genus *Mandrillus*.

The size similarities between the labyrinths of *Papio*, *Theropithecus*, *Mandrillus*, the male *Erythrocebus patas*, and the fossil *Paradolichopithecus* from Dafnero-3 clearly reflect the fact that they are all large cercopithecines (Fleagle, 1999; Kostopoulos *et al*., 2018). Within each Papionini subtribe, species with larger labyrinth size (*T. gelada*, *Papio* sp., *Mandrillus* sp. in Papionina, and *M. mulatta*, *M. sylvanus* in Macacina) are also those with less arboreal behavior, whereas species with the smallest labyrinth sizes (*L. albigena*, *M. fascicularis*) tend to be arboreal climbers — a trend probably linked to differences in body mass. The large labyrinth size of *Paradolichopithecus* supports post-cranial evidence of terrestrial behavior (Sondaar *et al*., 2006; Ting *et al*., 2004). The regression score for *Paradolichopithecus* corresponds to a large Cercopithecini, but it is not consistent with the extrapolation of shape for a large macaque. Therefore, the shape similarities between the fossil taxa and Macacina are more likely to reflect the retaining of several shape features that would represent the ancestral pattern for all Papionini and even all Cercopithecinae (as these features are also found in Cercopithecini), rather than the consequence of allometric shape changes in large Macacina.

The separation of each species is quite efficient when the shape of the whole labyrinth is used, contrary to previous studies based only on the shape of the semicircular canals, in which more overlap was observed (Beaudet *et al*., 2016). When considering the four first components of Procrustes shape coordinates, the separation between Papionini and Cercopithecini on the one hand, and between Macacina and Papionina on the other hand, is consistent with the classification of cercopithecines (Tosi *et al*., 2003). The separation between Papionina and the two other clades is partly driven by the allometric component, as it tends to be less good when this component is removed. The shape similarities between *Theropithecus* and *Lophocebus*, together with *Papio*, and the proximity of *Cercocebus* and *Mandrillus* also fit with the most recent phylogenies (Harris, 2000; Pugh & Gilbert, 2018; Tosi *et al*., 2003). These observations confirm that, even though the phylogenetic signal is weak, the labyrinth morphology as a whole provides some phylogenetic information at least at higher taxonomic levels (tribe, subtribe), as is observed for the semicircular canals alone (Beaudet *et al*., 2016; Urciuoli *et al*., 2020). The morphological affinities of *Paradolichopithecus* with Papionina regarding labyrinth shape speak in favour of closest phylogenetic relationships with this group, contrary to the classical hypothesis for a *Paradolichopithecus*–Macacina grouping. All clustering analyses show morphological affinities between *Paradolichopithecus* and *Mandrillus sphinx*; however, as these analyses tend to reflect size rather and not just phylogeny, it is still not clear whether this fossil belongs to the *Cercocebus*–*Mandrillus* clade, or to the *Papio*–*Theropithecus*–*Lophocebus* clade, or branches at a more basal position within Papionina or even Papionini.

Morphological similarities of the LGPUT DFN3-150 with Papionina are partially linked to centroid size of the bony labyrinth through allometric shape changes. This is visible in the clustering analyses, in which the dendrograms are less consistent with the known phylogeny when log centroid size is regressed out. The slightly weaker phylogenetic signal for regression residuals compared to Procrustes shape

Table IV Summary of the hypotheses regarding the bony labyrinth of Cercopithecinae

Hypotheses		Validity
H1	**Size is the main component of morphological variation** Support: - There is a very large centroid size variation across species - Heavier primates have larger centroid sizes	**Yes**
H2	**Allometry is an important component of shape variation** Contradiction (allometry present, but weak): - Shape variation is associated with labyrinth size variation and body mass, but the correlations are weak - The shape differences associated with the first four PCs are not the same as the allometric shape changes, except for PC4 (only 7.7% of the total variance)	**No, only little**
H3	**Morphology reflects both phylogeny and ecology** Support for phylogeny (at the subtribe level): - The rate of successful classification is good for the bgPCA - Clustering analyses on Procrustes shape coordinates roughly separate Macacina, Papionina and Cercopithecini - There is a phylogenetic signal in labyrinth shape - When a larger taxonomic range is considered (subfamily Cercopithecinae vs. tribe Papionini), the phylogenetic signal is slightly stronger for centroid size Contradiction with phylogeny (fine phylogenetic pattern): - Clustering analyses perform poorly for the fine phylogenetic patterning within each subtribe - The phylogenetic signal in labyrinth shape is weak = > adaptive signal?	**Probably yes**
H4	**The phylogenetic signal in the bony labyrinth morphology is mainly driven by size** Support (effect of size through allometry): - Species clustering in subtribes is less consistent when centroid size is regressed out - The phylogenetic signal is weaker when centroid size is regressed out - All PCs showing some separation between clades are weakly correlated with centroid size Contradiction (no direct effect of size): - The phylogenetic signal is weaker for centroid size, compared to Procrustes shape coordinates	**No, only weakly**

coordinates also points to a similar direction, although the difference remains small. Therefore, we can not exclude that the shape affinities of *Paradolichopithecus* with the baboon-related clade are the result of a parallel evolution for large, terrestrial species that would arise from a common allometric pattern across all cercopithecines (e.g., Nishimura *et al*., 2019). The Blomberg's K and K_{mult} values, which are all inferior to one, show that morphological variance is accumulated within clades, which is consistent with homoplasy. Though, labyrinth morphology does not depend just on CS, but also on phylogeny independently of body size. Indeed, Cercopithecini are separated from Macacina in the allometry-free shape space (with Papionina partially overlapping both of these clades at an intermediate position). This result is consistent with two recent analyses based on two different geometric morphometric protocols (Morimoto *et al*., 2020; Urciuoli *et al*., 2020).

The discrepancy between an absent or very weak signal for the phylogenetic and clustering analyses of allometry-free shape, and the good classification rates for the between-group principal component analysis, might be explained by two factors. First, the clustering analysis is based on Euclidean distances, which correspond to one variable summarizing many morphological traits. Therefore, the absence of clusters exactly similar to the molecular phylogeny does not necessarily mean that morphology does not reflect phylogeny. It only implies that the phylogenetic signal is not captured by the Euclidean distance, *taken alone*. Second, the bgPCA separates groups at high taxonomic levels (tribe, subtribe), whereas the phylogenetic and clustering analyses take into account the species level. We can interpret this as follows: when allometric effects are removed, labyrinth shape reflects phylogenetic patterns at relatively high taxonomic levels (subtribe or above), but not necessarily at lower levels, which is consistent with recent findings for anthropoids (Beaudet *et al.*, 2016; del Rio *et al.*, 2021; Morimoto *et al.*, 2020; Urciuoli *et al.*, 2020). As a consequence, the position of the fossil in the allometry-free shape space is likely to reflect a phylogenetic proximity with Papionina as a group, but it cannot be used to infer its affinities with any particular extant species within this group.

Because our results demonstrate that the correlation between labyrinth shape (not size) and body mass is only weak in Cercopithecinae, we would recommend to relying more on this feature to infer phylogeny at a large taxonomical scale, rather than the outer cranial features which are known to be highly correlated with body mass and ecology. However at lower taxonomical scales, both types of evidence might be as useful, since labyrinth morphology does not seem to perform particularly well to infer the fine phylogenetic pattern. This could be explained by the fact that labyrinth morphology is also associated with cranial base shape (Jeffery & Spoor, 2004; Le Maître, 2019; Spoor & Zonneveld, 1998), which depends on body mass and ecology.

The rough morphological resemblance of some young *Paradolichopithecus* individuals, such as LGPUT DFN3-150, with *Macaca* could be justified by the similar pre-adult ontogenetic trajectories followed by male and female macaques, mandrills, mangabeys, and baboons (Leigh, 2006; Mottura & Gentili, 2006). Taking into account all these elements, together with the findings of the present study, a hypothesis of *Paradolichopithecus* – Papionina relationship appears more supported than the traditional *Paradolichopithecus* – Macacina one. An alternative hypothesis would be that *Paradolichopithecus* was a basal Papionini, closer to Papionina relative to Macacina, sharing common shape features with both groups because of common ancestry and convergent allometric pattern for all Cercopithecinae. This hypothesis might be ruled out with further analyses conducted on basal African Papionini, which is beyond the scope of the present paper.

Concluding remarks

Our results confirm that, even using a small number of landmarks, the morphology of the bony labyrinth can be used to infer phylogenetic relationships of primate species. However, as highlighted in other studies, it is reliable only at taxonomic

levels higher than the family. As in other primate groups, we found an important size variation, which is the main driver of the phylogenetic signal in labyrinth morphology. Surprisingly, despite this large size variation, allometry is only a minor component of labyrinth shape variation in Cercopithecinae. This is a large aspect for the reconstruction of phylogenetic affinities of other fossil papionins, as the main issue in this group is generally to disentangle the phylogenetic and the allometric components in morphological features. Our findings do not provide a clear answer to the taxonomic classification of *Paradolichopithecus*, though the traditional hypothesis of a *Paradolichopithecus* –Macacina relationship appears to be the least supported. In any case, the results of the present study reveal that the evolutionary history of Eurasian late Neogene–Quaternary cercopithecids might be more complicated than previously thought, and point to the need for a fresh in-depth phylogenetic investigation.

References

Adams, D. C. (2014). A generalized K statistic for estimating phylogenetic signal from shape and other high-dimensional multivariate data. *Systematic Biology, 63*, 685–697. https://doi.org/10.1093/sysbio/syu030

Adams, D. C., Collyer, M. L., Kaliontzopoulou, A, et al. (2021). *geomorph: software for geometric morphometric analyses*. R package version 4.0.0. https://cran.r-project.org/package=geomorph

Aguirre, E., Vangengeim, E. A., Morales, J., et al. (1994). Plio-Pleistocene mammal faunas: an overview. In J. van Couvering (Ed.), *The Pleistocene boundary and the beginning of the quaternary* (pp. 114–128). Cambridge UK: Cambridge University Press

Agusti, J., & Antón, M. (2002). *Mammoths, sabertooths, and hominids; 65 million years of mammalian evolution in Europe*. Columbia University Press

Arnold, C., Matthews, L. J., & Nunn, C. L. (2010). The 10kTrees website: A new online resource for primate phylogeny. *Evolutionary Anthropology, 19*, 114–118. https://doi.org/10.1002/evan.20251

Baken, E. K., Collyer, M. L., Kaliontzopoulou, A., et al. (2021). geomorph v4.0 and gmShiny: Enhanced analytics and a new graphical interface for a comprehensive morphometric experience. *Methods in Ecology and Evolution, 12*, 2355–2363. https://doi.org/10.1111/2041-210X.13723

Baker, W. E., & Durand, H. M. (1836). Fossil remains of smaller Carnivora from the Sub-Himalayas. *Journal of the Asiatic Society of Bengale, 5*, 565–570

Beaudet, A., Dumoncel, J., Thackeray, F., et al. (2016). upper third molar internal structural organization and semicircular canal morphology in Plio-Pleistocene South African cercopithecoids. *Journal of Human Evolution, 95*, 104–120. https://doi.org/10.1016/j.jhevol.2016.04.004

Beaudet, A., Dumoncel, J., Thackeray, F., et al. (2019). 3D models related to the publication: Upper upper third molar internal structural organization and semicircular canal morphology in Plio-Pleistocene South African cercopithecoids. *MorphoMuseuM*, 5, e86. https://doi.org/10.18563/journal.m3.86.

Blomberg, S. P., Garland, T., & Ives, A. R. (2003). Testing for phylogenetic signal in comparative data: behavioral traits are more labile. *Evolution, 57*, 717–745. https://doi.org/10.1111/j.0014-3820.2003.tb00285.x

Bookstein, F. L. (1991). *Morphometric tools for landmark data: geometry and biology*. Cambridge UK: Cambridge University Press.

Bookstein, F. L. (2019). Pathologies of between-groups principal components analysis in geometric morphometrics. *Evolutionary Biology, 46*, 271–302. https://doi.org/10.1007/s11692-019-09484-8

Boucherie, A., Polet, C., Lefèvre, P., & Vercauteren, M. (2021). Sexing the bony labyrinth: a morphometric investigation in a subadult and adult Belgian identified sample. *Journal of Forensic Sciences, 66*, 808–820. https://doi.org/10.1111/1556-4029.14663

Boulesteix, A. L. (2005). A note on between-group PCA. *International Journal of Pure and Applied Mathematics, 19*, 359–366. https://doi.org/10.5282/ubm/epub.1767

Cardini, A., & Polly, P. D. (2020). Cross-validated between group PCA scatterplots: a solution to spurious group separation? *Evolutionary Biology, 47*, 85–95. https://doi.org/10.1007/s11692-020-09494-x

Copes, L. E., & Kimbel, W. H. (2016). Cranial vault thickness in primates: *homo erectus* does not have uniquely thick vault bones. *Journal of Human Evolution, 90*, 120–134. https://doi.org/10.1016/j.jhevol.2015.08.008

Copes, L. E., Lucas, L. M., Thostenson, J. O., et al. (2016). A collection of non-human primate computed tomography scans housed in MorphoSource, a repository for 3D data. *Scientific Data, 3*, 160001. https://doi.org/10.1038/sdata.2016.1

Delson, E., & Frost, S. R. (2004). *Paradolichopithecus*: A large-bodied terrestrial papionin (Cercopithecidae) from the Pliocene of western Eurasia. *American Journal of Physical Anthropology*, 38(Suppl.), 85

Delson, E., Terranova, C. J., Jungers, W. L., Sargis, E. J., & Jablonski, N. G. (2000). Body mass in Cercopithecidae (Primates, Mammalia): estimation and scaling in extinct and extant taxa. *Anthropological papers of the AMNH* (Vol. 83). American Museum of Natural History

Drake, A. G., & Klingenberg, C. P. (2008). The pace of morphological change: Historical transformation of skull shape in St Bernard dogs. *Proceedings of the Royal Society b: Biological Sciences, 275*(1630), 71–76. https://doi.org/10.1098/rspb.2007.1169

Ekdale, E. G. (2016). Form and function of the mammalian inner ear. *Journal of Anatomy, 228*, 324–337. https://doi.org/10.1111/joa.12308

Eronen, J. T., & Rook, L. (2004). The Mio-Pliocene European primate fossil record: Dynamics and habitat tracking. *Journal of Human Evolution, 47*, 323–341. https://doi.org/10.1016/j.jhevol.2004.08.003

Fleagle, J. G. (1999). *Primate Adaptation and Evolution*. San Diego CA: Elsevier Academic Press

Frost, S. R., Marcus, L. F., Bookstein, F. L., et al. (2003). Cranial allometry, phylogeography, and systematics of large-bodied papionins (Primates: Cercopithecinae) inferred from geometric morphometric analysis of landmark data. *The Anatomical Record, 275*, 1048–1072. https://doi.org/10.1002/ar.a.10112

Georgi, J. A. (2008) *Semicircular canal morphology as evidence of locomotor environment in amniotes*. Dissertation, Stony Brook University

Gilbert, C. C., Frost, S. R., & Strait, D. S. (2009). Allometry, sexual dimorphism, and phylogeny: A a cladistic analysis of extant African papionins using craniodental data. *Journal of Human Evolution, 57*(3), 298–320. https://doi.org/10.1016/j.jhevol.2009.05.013

Gilbert, C. C., & Rossie, J. B. (2007). Congruence of molecules and morphology using a narrow allometric approach. *Proceedings of the National Academy of Sciences of the United States of America, 104*(29), 11910–11914. https://doi.org/10.1073/pnas.0702174104

Gonzales, L. A., Malinzak, M. D., & Kay, R. F. (2019). Intraspecific variation in semicircular canal morphology — a missing element in adaptive scenarios? *American Journal of Physical Anthropology, 168*(1), 10–24. https://doi.org/10.1002/ajpa.23692

Graf, W., & Klam, F. (2006). Le système vestibulaire: Anatomie fonctionnelle et comparée, évolution et développement. *Comptes Rendus Palevol, 5*(3), 637–655. https://doi.org/10.1016/j.crpv.2005.12.009

Grohé, C., Tseng, Z. J., Lebrun, R., et al. (2016). Bony labyrinth shape variation in extant Carnivora: A case study of Musteloidea. *Journal of Anatomy, 228*, 366–383. https://doi.org/10.1111/joa.12421

Gunz, P., Ramsier, M., Kuhrig, M., et al. (2012). The mammalian bony labyrinth reconsidered, introducing a comprehensive geometric morphometric approach. *Journal of Anatomy, 220*, 529–543. https://doi.org/10.1111/j.1469-7580.2012.01493.x

Harris, E. E. (2000). Molecular systematics of the Old World monkey tribe Papionini: analysis of the total available genetic sequences. *Journal of Human Evolution, 38*, 235–256. https://doi.org/10.1006/jhev.1999.0318

Hermier, R., Merceron, G., & Kostopoulos, D. S. (2020). The emblematic Eurasian Villafranchian antelope *Gazellospira* (Mammalia: Bovidae): new insights from the Lower Pleistocene Dafnero fossil sites (Northern Greece). *Geobios, 61*, 11–29. https://doi.org/10.1016/j.geobios.2020.06.006

Jablonski, N. G. (2002). Fossil Old World monkeys: The late Neogene radiation. In W. C. Hartwig (Ed.), *The Primate Fossil Record* (pp. 255–299). Cambridge UK: Cambridge University Press

Jeffery, N., & Spoor, F. (2004). Prenatal growth and development of the modern human labyrinth. *Journal of Anatomy, 204*, 71–92. https://doi.org/10.1111/j.1469-7580.2004.00250.x

Joganic, J. L., & Heuzé, Y. (2019). Allometry and advancing age significantly structure craniofacial variation in adult female baboons. *Journal of Anatomy, 235*(2), 217–232. https://doi.org/10.1111/joa.13005

Joganic, J. L., Willmore, K. E., Richtsmeier, J. T., et al. (2018). Additive genetic variation in the craniofacial skeleton of baboons (genus *Papio*) and its relationship to body and cranial size. *American Journal of Physical Anthropology, 165*, 269–285. https://doi.org/10.1002/ajpa.23349

Jolly, C. J. (1967). The evolution of baboons. In H. Vagtborg (Ed.), *The Baboon in medical research* (Vol. 2, pp. 23–50). Austin: University of Texas Press

Kostopoulos, D. S., Guy, F., Kynigopoulou, Z., et al. (2018). A 2Ma old baboon-like monkey from Northern Greece and new evidence to support the *Paradolichopithecus — Procynocephalus* synonymy (Primates: Cercopithecidae). *Journal of Human Evolution, 121*, 178–192. https://doi.org/10.1016/j.jhevol.2018.02.012

Koufos, G. D. (2001). The Villafranchian mammalian faunas and biochronology of Greece. *Bollettino-Societa Paleontologica Italiana, 40*(2), 217–223

Koufos, G. D., Kostopoulos, D. S., & Merceron, G. (2020). The saber-toothed cat *Homotherium latidens* (Owen, 1846) from the lower Pleistocene locality Dafnero, Western Macedonia, Greece. *Geodiversitas, 42*(10), 139–149. https://doi.org/10.5252/geodiversitas2020v42a10

Le Maître, A. (2019). The role of spatial integration in the morphology of the bony labyrinth in modern humans. *BMSAP, 31*, 34–42. https://doi.org/10.3166/bmsap-2018-0039

Le Maître, A., Schuetz, P., Vignaud, P., et al. (2017). New data about semicircular canal morphology and locomotion in modern hominoids. *Journal of Anatomy, 231*, 95–109. https://doi.org/10.1111/joa.12619

Lebrun, R., Godinot, M., Couette, S., et al. (2012). The labyrinthine morphology of *Pronycticebus gaudryi* (Primates, Adapiformes). *Palaeobiodiversity and Palaeoenvironments, 92*(4), 527–537. https://doi.org/10.1007/s12549-012-0099-z

Lebrun, R., Perier, A., Masters, J., Marivaux, L., & Couette, S. (2021). Lower levels of vestibular developmental stability in slow-moving than fast-moving primates. *Symmetry*, 13(12). https://doi.org/10.3390/sym13122305.

Lebrun, R., Ponce de León, M. S., Tafforeau, P., et al. (2010). Deep evolutionary roots of strepsirrhine primate labyrinthine morphology. *Journal of Anatomy, 216*, 368–380. https://doi.org/10.1111/j.1469-7580.2009.01177.x

Leigh, S. R. (2006). Cranial ontogeny of *Papio* baboons (*Papio hamadryas*). *American Journal of Physical Anthropology, 130*, 71–84. https://doi.org/10.1002/ajpa.20319

Leigh, S. R., Shah, N. F., & Buchanan, L. S. (2003). Ontogeny and phylogeny in papionin primates. *Journal of Human Evolution, 45*, 285–316. https://doi.org/10.1016/j.jhevol.2003.08.004

Maier, W. (2013). The entotympanic in late fetal artiodactyla (Mammalia). *Journal of Morphology, 274*, 926–939. https://doi.org/10.1002/jmor.20149

Maschenko, E. N. (1994). Comparative morphological analysis of the skull and lower jaw of the late Pliocene baboon *Papio suschkini*. In L. P. Tatarinov (Ed.), *Paleonteriologia* (pp. 15–57). Nauka. (in Russian)

Maschenko, E. N. (2005). Cenozoic primates of eastern Eurasia (Russia and adjacent areas). *Anthropological Science, 113*, 103–115. https://doi.org/10.1537/ase.04S015

Mejdoubi, M., Dedouit, F., Mokrane, F. Z., & Telmon, N. (2015). Semicircular canal angulation during fetal life: A computed tomography study of 54 human fetuses. *Otology & Neurotology, 36*(4), 701–704. https://doi.org/10.1097/MAO.0000000000000640

Mejdoubi, M., Dedouit, F., Mokrane, F. Z., & Telmon, N. (2016). CT scan imaging of the human fetal labyrinth: Case series data throughout gestation. *Otology & Neurotology, 37*(5), 602–607. https://doi.org/10.1097/MAO.0000000000001039

Mennecart, B., & Costeur, L. (2016). Shape variation and ontogeny of the ruminant bony labyrinth, an example in Tragulidae. *Journal of Anatomy, 229*, 422–435. https://doi.org/10.1111/joa.12487

Mitteroecker, P., & Bookstein, F. (2011). Linear discrimination, ordination, and the visualization of selection gradients in modern morphometrics. *Evolutionary Biology, 38*, 100–114. https://doi.org/10.1007/s11692-011-9109-8

Mitteroecker, P., Gunz, P., Windhager, S., et al. (2013). A brief review of shape, form, and allometry in geometric morphometrics, with applications to human facial morphology. *Hystrix, Italian Journal of Mammalogy, 24*(1), 59–66. https://doi.org/10.4404/hystrix-24.1-6369

Monson, T. A., Brasil, M. F., Stratford, D. J., et al. (2017) Patterns of craniofacial variation and taxonomical diversity in the South African Cercopithecidae fossil record**.** *Palaeontologia Electronica*, 20.1.7A, 1–20. https://doi.org/10.26879/690

Morimoto, N., Kunimatsu, Y., Nakatsukasa, M., et al. (2020). Variation of bony labyrinthine morphology in Mio-Plio-Pleistocene and modern anthropoids. *American Journal of Physical Anthropology, 173*(2), 276–292. https://doi.org/10.1002/ajpa.24098

Mottura, A., & Gentili, S. (2006). Cranio e mandibular biometrics and skull maturation of *Macaca sylvanus* L., 1758. *Journal of Human Evolution, 21*, 223–239. https://doi.org/10.1007/s11598-006-9020-y

Murdoch, D., & Adler, D. (2021). rgl: 3D visualization using Open GL. R package version 0.107.14. https://CRAN.R-project.org/package=rgl

Nishimura, T. D., Ito, T., Yano, W., et al. (2014). Nasal architecture in *Procynocephalus wimani* (Early Pleistocene, China) and implications for its phyletic relationship with *Paradolichopithecus*. *Anthropological Science,* 122, 101–113. https://doi.org/10.1537/ase.140624

Nishimura, T. D., Morimoto, N., & Ito, T. (2019). Shape variation in the facial part of the cranium in macaques and African papionins using geometric morphometrics. *Primates, 60*(5), 401–418. https://doi.org/10.1007/s10329-019-00740-1

Nishimura, T. D., Zhang, Y., & Takai, M. (2010). Nasal anatomy of *Paradolichopithecus gansuensis* (Early Pleistocene, Longdan, China) with comments on phyletic relationships among the species of this genus. *Folia Primatologica, 81*(2), 53–62. https://doi.org/10.1159/000284585

O'Shea, N., Delson, E., Pugh, K. D., et al. (2016). Phylogenetic analysis of *Paradolichopithecus*: Fossil baboon or macaque? Program of the 85th Annual Meeting of the American Association of Physical Anthropology. *American Journal of Physical Anthropology, 159*, 244. https://doi.org/10.1002/ajpa.22955

Paradis, E., & Schliep, K. (2019). ape 5.0: An environment for modern phylogenetics and evolutionary analyses in R. *Bioinformatics, 35*, 526–528. https://doi.org/10.1093/bioinformatics/bty633

Perier, A., Lebrun, R., & Marivaux, L. (2016). Different level of intraspecific variability of the bony labyrinth morphology in slow- versus fast-moving primates. *Journal of Mammalian Evolution, 23*, 353–368. https://doi.org/10.1007/s10914-016-9323-3

Pfaff, C., Martin, T., & Ruf, I. (2015). Bony labyrinth morphometry indicates locomotor adaptations in the squirrel-related clade (Rodentia, Mammalia. *Proceedings of the Royal Society b: Biological Sciences, 282*(1809), 20150744. https://doi.org/10.1098/rspb.2015.0744

Plastiras Ch.-A. (2021). *Ecological diversity of Pliocene to Pleistocene Palaearctic cercopithecids (Primates, Mammalia); evidence from the dental tissue.* PhD Thesis, Aristotle University of Thessaloniki. 238 pp.

Popescu, S.-M., Biltekin, D., Winter, H., et al. (2010). Pliocene and Lower Pleistocene vegetation and climate changes at the European scale: long pollen records and climatostratigraphy. *Quaternary International, 219*(1–2), 152–167. https://doi.org/10.1016/j.quaint.2010.03.013

Profico, A., Piras, P., Buzi, C., Di Vincenzo, F., Lattarini, F., Melchionna, M., … Manzi, G. (2017). The evolution of cranial base and face in Cercopithecoidea and Hominoidea: Modularity and morphological integration. *American Journal of Primatology*, 79(12), e22721–n. https://doi.org/10.1002/ajp.22721.

Pugh, K. D., & Gilbert, C. C. (2018). Phylogenetic relationships of living and fossil African papionins: Combined evidence from morphology and molecules. *Journal of Human Evolution, 123*, 35–51. https://doi.org/10.1016/j.jhevol.2018.06.002

Qiu, Z., Deng, T., & Wang, B. (2004). Early Pleistocene mammalian fauna from Longdan, Dongxiang, Gansu, China. *Palaeontologia Sinica, 27*, 1–798. (in Chinese with English summary)

R Development Core Team. (2021). *R: A language and environment for statistical computing.* R Foundation for Statistical Computing, Vienna, Austria. URL https://www.R-project.org/.

Radović, P., Lindal, J., Marković, Z., et al. (2019). First record of a fossil monkey (Primates, Cercopithecidae) from the Late Pliocene of Serbia. *Journal of Human Evolution, 137*, 102681. https://doi.org/10.1016/j.jhevol.2019.102681

Rae, T. C. (2008). Paranasal pneumatization in extant and fossil Cercopithecoidea. *Journal of Human Evolution, 54*, 279–286. https://doi.org/10.1159/000449286

Rae, T. C., Johnson, P. M., Yano, W., & Hirasaki, E. (2016). Semicircular canal size and locomotion in colobine monkeys: a cautionary tale. *Folia Primatologica, 87*(4), 213–223. https://doi.org/10.1159/000449286

del Rio, J., Aristide, L., dos Reis, S. F., et al. (2021). Allometry, function and shape diversification in the inner ear of platyrrhine primates. *Journal of Mammalian Evolution, 28*, 135–143. https://doi.org/10.1007/s10914-019-09490-9

Rohlf, F. J., & Slice, D. (1990). Extensions of the Procrustes method for the optimal superimposition of landmarks. *Systematic Zoology, 39*, 40–59. https://doi.org/10.2307/2992207

Ryan, T. M., Silcox, M. T., Walker, A., et al. (2012). Evolution of locomotion in Anthropoidea: The semicircular canal evidence. *Proceedings of the Royal Society B: Biological Sciences, 279*(1742), 3467–3475. https://doi.org/10.1098/rspb.2012.0939

Saitou, N., & Nei, M. (1987). The neighbor-joining method: A new method for reconstructing phylogenetic trees. *Molecular Biology and Evolution, 4*(4), 406–425. https://doi.org/10.1093/oxfordjournals.molbev.a040454

Schlager, S. (2017). Morpho and Rvcg — Shape analysis in R: R-packages for geometric morphometrics, shape analysis and surface manipulations. In G. Zheng, S. Li, & G. Szekely (Eds.), *Statistical shape and deformation analysis: methods, implementation and applications* (pp. 217–256). San Diego CA: Academic Press

Schwab, J. A., Kriwet, J., Weber, G. W., et al. (2019). Carnivoran hunting style and phylogeny reflected in bony labyrinth morphometry. *Scientific Reports, 9*(1), 70. https://doi.org/10.1038/s41598-018-37106-4

Silcox, M. T., Bloch, J. I., Boyer, D. M., et al. (2009). Semicircular canal system in early primates. *Journal of Human Evolution, 56*, 315–327. https://doi.org/10.1016/j.jhevol.2008.10.007

Singleton, M. (2002). Patterns of cranial shape variation in the Papionini (Primates: Cercopithecinae). *Journal of Human Evolution, 42*, 547–578. https://doi.org/10.1006/jhev.2001.0539

Sondaar, P. Y., van der Geer, A. A. E., & Dermitzakis, M. D. (2006). The unique postcranial of the Old World monkey *Paradolichopithecus*: More similar to *Australopithecus* than to baboons. *Hellenic Journal of Geosciences, 41*(1), 19–28

Sotnikova, M., & Rook, L. (2010). Dispersal of the Canini (Mammalia, Canidae: Caninae) across Eurasia during the Late Miocene to Early Pleistocene. *Quaternary International, 212*(2), 86–97. https://doi.org/10.1016/j.quaint.2009.06.008

Spoor, C. F. (1993). *The comparative morphology and phylogeny of the human bony labyrinth*. Dissertation, Universiteit Utrecht, Faculteit Geneeskunde

Spoor, F., & Zonneveld, F. (1998). Comparative review of the human bony labyrinth. *American Journal of Physical Anthropology, 107*, 211–251. https://doi.org/10.1002/(SICI)1096-8644(1998)107:27+%3C211::AID-AJPA8%3E3.0.CO;2-V

Spoor, F., Wood, B., & Zonneveld, F. (1994). Implications of early hominid labyrinthine morphology for evolution of human bipedal locomotion. *Nature, 369*, 645–648. https://doi.org/10.1038/369645a0

Spoor, F., Wood, B., & Zonneveld, F. (1996). Evidence for a link between human semicircular canal size and bipedal behaviour. *Journal of Human Evolution, 30*, 183–187. https://doi.org/10.1006/jhev.1996.0018

Spoor, F., Garland, T., Krovitz, G., et al. (2007). The primate semicircular canal system and locomotion. *Proceedings of the National Academy of Sciences of the United States of America, 104*, 10808–10812. https://doi.org/10.1073/pnas.0704250104

Strasser, E., & Delson, E. (1987). Cladistic analysis of cercopithecid relationships. *Journal of Human Evolution, 16*, 81–99. https://doi.org/10.1016/0047-2484(87)90061-3

Szalay, F. S., & Delson, E. (1979). *Evolutionary history of the Primates*. Academic Press

Takai, M., Maschenko, E. N., Nishimura, T. D., et al. (2008). Phylogenetic relationships and biogeographic history of Paradolichopithecus sushkini Trofimov 1977, a large-bodied cercopithecine monkey from the Pliocene of Eurasia. *Quaternary International, 179*(1), 108–119. https://doi.org/10.1016/j.quaint.2007.10.012

Takai, M., Zhang, Y., Kono, R. T., et al. (2014). Changes in the composition of the Pleistocene primate fauna in southern China. *Quaternary International, 354*, 75–85. https://doi.org/10.1016/j.quaint.2014.02.021

Ting, N., Harcourt-Smith, W. E. H., Frost, S. R., et al. (2004). Description and analysis of postcranial elements of *Paradolichopithecus arvernensis*: a large bodied papionin from the Pliocene of Eurasia. *American Journal of Physical Anthropology*, 38 (Suppl.), 195

Tosi, A. J., Disotell, T. R., Morales, J. C., et al. (2003). Cercopithecine Y-chromosome data provide a test of competing morphological evolutionary hypotheses. *Molecular Phylogenetics and Evolution, 27*(3), 510–521. https://doi.org/10.1016/S1055-7903(03)00024-1

Urciuoli, A., Zanolli, C., Beaudet, A., et al. (2020). The evolution of the vestibular apparatus in apes and humans. *eLife, 9*, e51261. https://doi.org/10.7554/eLife.51261

Urciuoli, A., & Zanolli, C. (2021). Reassessment of the phylogenetic relationships of the late Miocene apes *Hispanopithecus* and *Rudapithecus* based on vestibular morphology. *Proceedings of the National Academy of Sciences of the United States of America, 118*(5), e2015215118. https://doi.org/10.1073/pnas.2015215118

van der Geer, A. A. E., & Sondaar, P. Y. (2002). The postcranial elements of *Paradolichopithecus arvernensis* (Primates, Cercopithecidae, Papionini) from Lesvos, Greece. *Annales Géologiques Des Pays Helléniques, 39*, 71–86

Venables, W. N., & Ripley, B. D. (2002). *Modern Applied Statistics with S* (4th ed.). New York: Springer

Walker, A., Ryan, T. M., Silcox, M. T., et al. (2008). The semicircular canal system and locomotion: The case of extinct lemuroids and lorisoids. *Evolutionary Anthropology: Issues, News, and Reviews, 17*(3), 135–145. https://doi.org/10.1002/evan.20165

Williams, F., & Holmes, N. (2012). Dental microwear texture analysis of late Pliocene *Procynocephalus subhimalayanus* (Primates: Cercopithecidae) of the Upper Siwaliks, India. *Open Geosciences, 4*(3), 425–438. https://doi.org/10.2478/s13533-011-0076-5

Wilson, S. R. (1981). On comparing fossil specimens with population samples. *Journal of Human Evolution, 10*(3), 207–214. https://doi.org/10.1016/S0047-2484(81)80059-0